

## Ethanol gas sensing properties of Al<sub>2</sub>O<sub>3</sub>-doped ZnO thick film resistors

D R PATIL, L A PATIL\* and D P AMALNERKAR<sup>†</sup>

Materials Research Lab, Pratap College, Amalner 425 401, India

<sup>†</sup>Centre for Materials for Electronics Technology, Pune 411 008, India

MS received 13 July 2007

**Abstract.** The characterization and ethanol gas sensing properties of pure and doped ZnO thick films were investigated. Thick films of pure zinc oxide were prepared by the screen printing technique. Pure zinc oxide was almost insensitive to ethanol. Thick films of Al<sub>2</sub>O<sub>3</sub> (1 wt%) doped ZnO were observed to be highly sensitive to ethanol vapours at 300°C. Aluminium oxide grains dispersed around ZnO grains would result into the barrier height among the grains. Upon exposure of ethanol vapours, the barrier height would decrease greatly leading to drastic increase in conductance. It is reported that the surface misfits, calcination temperature and operating temperature can affect the microstructure and gas sensing performance of the sensor. The efforts are, therefore, made to create surface misfits by doping Al<sub>2</sub>O<sub>3</sub> into zinc oxide and to study the sensing performance. The quick response and fast recovery are the main features of this sensor. The effects of microstructure and additive concentration on the gas response, selectivity, response time and recovery time of the sensor in the presence of ethanol vapours were studied and discussed.

**Keywords.** Al<sub>2</sub>O<sub>3</sub> doped ZnO; ethanol gas sensor; thick film; gas response.

### 1. Introduction

Semiconducting oxides are widely used as inexpensive and robust sensors for toxic, hazardous and combustible gases and vapours in safety and automotive applications. Few semiconducting oxides used in these applications are ZnO, SnO<sub>2</sub> (Seiyama *et al* 1962; Seiyama and Era 1971; Moseley 1992), Fe<sub>2</sub>O<sub>3</sub> (Patil and Patil 2006a), CuO–SnO<sub>2</sub> (Patil and Patil 2006b), etc. Among all, ZnO is attracting considerable attention (Pearson *et al* 2005) for its possible applications in UV light emitters, spin functional devices, gas/odor sensors, transparent electronic devices and surface acoustic wave devices. ZnO has been utilized in a wide range of applications (Trivikrama Rao and Madhavendra 1995; Chaudhary *et al* 1999). Alumina (Al<sub>2</sub>O<sub>3</sub>)/Al<sup>3+</sup> has been studied and used as gas sensing element (Nanto *et al* 1993; Chang *et al* 2002). In fact, pure ZnO and Al<sub>2</sub>O<sub>3</sub> thick films were reported to have poor gas sensitivity.

Ethanol is explosively utilized for beverages, industrial and scientific sectors. Ethanol is a hypnotic (sleep producer) (Solomans and Fryhle 2004) gas having toxic nature. Heavy exposure and/or consumption of alcoholic beverages, particularly by smokers, increase the risk of cancer (Sodhi 2002) of the upper respiratory and digestive tracks. Alcoholic cirrhosis leads to liver cancer. Amongst the women, the chances of breast cancer increase with alco-

holic consumption or exposure. Those working on ethanol synthesis have great chances of being victims of respiratory and digestive track cancer. So there is a great demand and emerging challenges for monitoring ethanol gas at trace level.

The gas sensing performance of the material can be improved by incorporating few additives into the base material and/or surface activation (Matsushima *et al* 1989; Xiangfeng *et al* 2000) of thick films. The response of ZnO has been studied by various techniques such as spray pyrolysis deposition (Jayaraman *et al* 1999), thin films (Lin *et al* 1995), thick films (Patil and Patil 2006b), heterocontacts (Miyayama *et al* 1995), etc. Although few researchers have conducted studies on ethanol (Takao *et al* 1989; Miremadi *et al* 1994) gas sensors, it has not been possible to produce ethanol sensors in sufficient quantities to meet the demand.

The aim of the present work is to develop the sensor by modifying pure ZnO base material, which could be able to detect the C<sub>2</sub>H<sub>5</sub>OH vapours. Among the various metal oxide additives tested, Al<sub>2</sub>O<sub>3</sub> in ZnO is outstanding in promoting the sensing properties of C<sub>2</sub>H<sub>5</sub>OH in air.

### 2. Experimental

#### 2.1 Preparation of material powder

AR grade zinc oxide powder (99.9% pure) and aluminium chloride were mixed mechanochemically to obtain Al<sub>2</sub>O<sub>3</sub>-doped ZnO powders in various weight percentages such

\*Author for correspondence (lapresearch@rediffmail.com)

as 1, 3, 5, 7 and 9 wt%. Thus prepared powders were calcined at 700°C for 24 h in air and ball milled to ensure sufficiently fine particle size.

## 2.2 Preparation of thick films

The thixotropic pastes of pure and doped ZnO (Patil and Patil 2006b) were formulated by mixing the resulting fine powders with a solution of ethyl cellulose (a temporary binder) in a mixture of organic solvents such as butyl cellulose, butyl carbitol acetate and turpineol. The ratio of inorganic to organic part was kept as 75 : 25 in formulating the pastes. The thixotropic pastes were screen printed onto a glass substrate in desired patterns. The films so prepared were fired at 500°C for 24 h.

## 2.3 Characterization

The microstructure and chemical composition of the films were analysed using a scanning electron microscope (SEM, JEOL JED 2300) coupled with an energy dispersive spectrometer (EDS JEOL 6360 LA). Thickness measurements were carried out using a Taylor-Hobson (Talystep, UK) system. Electrical and gas sensing characteristics were measured using a static gas sensing system.

## 2.4 Details of gas sensing system

The sensing performance of the sensors was examined using a 'static gas sensing system' reported elsewhere (Patil *et al* 2006b).

## 3. Materials characterization

### 3.1 Thickness measurement

Thicknesses of the thick films were measured by using the Taylor-Hobson (Talystep, UK) system. The thicknesses of the films were observed in the range from 25–35  $\mu\text{m}$ . The reproducibility of the film thickness was achieved by maintaining proper rheology and thixotropy of the paste.

### 3.2 Structural properties (X-ray diffraction studies)

The crystalline structures of the films were analysed with X-ray diffractogram (RIGAKU DMAX 2500) using  $\text{CuK}\alpha$  radiation with a wavelength, 1.5418 Å.

Figure 1 depicts the XRD patterns of unmodified (pure) and  $\text{Al}_2\text{O}_3$  doped ZnO films. The observed peaks in figure 1(a) are matching well with ASTM reported data of ZnO. The peaks of the XRD pattern in figure 1(b) correspond to ZnO,  $\beta\text{-Al}_2\text{O}_3$  and  $\text{ZnAl}_2\text{O}_4$  materials and are observed to be microcrystalline in nature. The peaks of ZnO and  $\text{Al}_2\text{O}_3$  are indexed.

## 3.3 Elemental analysis

The quantitative elemental compositions of the pure and doped ZnO films were analysed using an energy dispersive spectrometer. The mass% of Zn and O in each samples were not as per the stoichiometric proportion and all samples were observed to be oxygen deficient. Excess or deficiency of the constituent material particles leads to the semiconducting nature of the material.

## 3.4 Microstructural analysis

Figure 2 depicts the SEM images of pure and  $\text{Al}_2\text{O}_3$ -doped ZnO films. Figure 2(a) depicts the microstructure of pure ZnO thick film. Figure 2(b) depicts the microstructure of  $\text{Al}_2\text{O}_3$  (1 wt%)-doped ZnO film. It is clear from this figure that the doping of  $\text{Al}_2\text{O}_3$  affected the microstructure of ZnO. The film consists of voids and grains with sizes ranging from 100–1500 nm distributed non-uniformly. Figure 2(c) depicts the microstructure of  $\text{Al}_2\text{O}_3$  (7 wt%)-doped ZnO film which consists of even smaller grains as compared to the grains associated with figure 2(b). Most of the grains of Zn-species are covered with smaller grains of Al-species, due to high agglomeration of Al-species. The films consist of voids and a wide range of grains with grain sizes ranging from 90–1400 nm distributed non-uniformly.

## 4. Electrical properties of sensor

### 4.1 $I$ - $V$ characteristics

Figure 3 depicts  $I$ - $V$  characteristics of  $\text{Al}_2\text{O}_3$  doped ZnO films. It is clear from the symmetrical nature of  $I$ - $V$  characteristics that the silver contacts on the films were ohmic in nature.

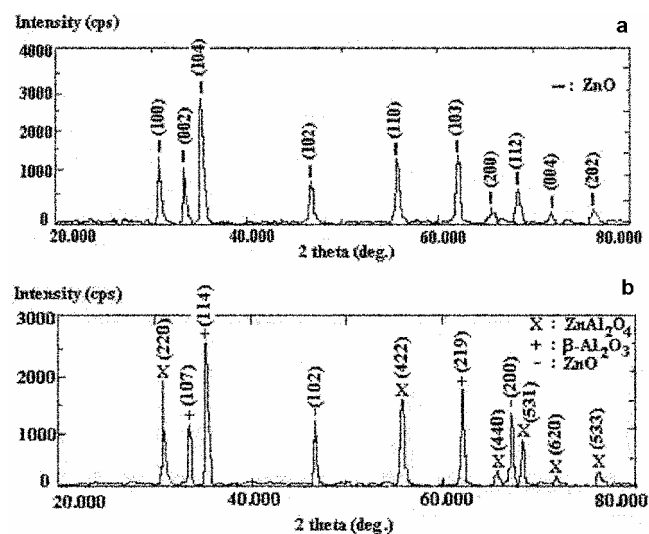
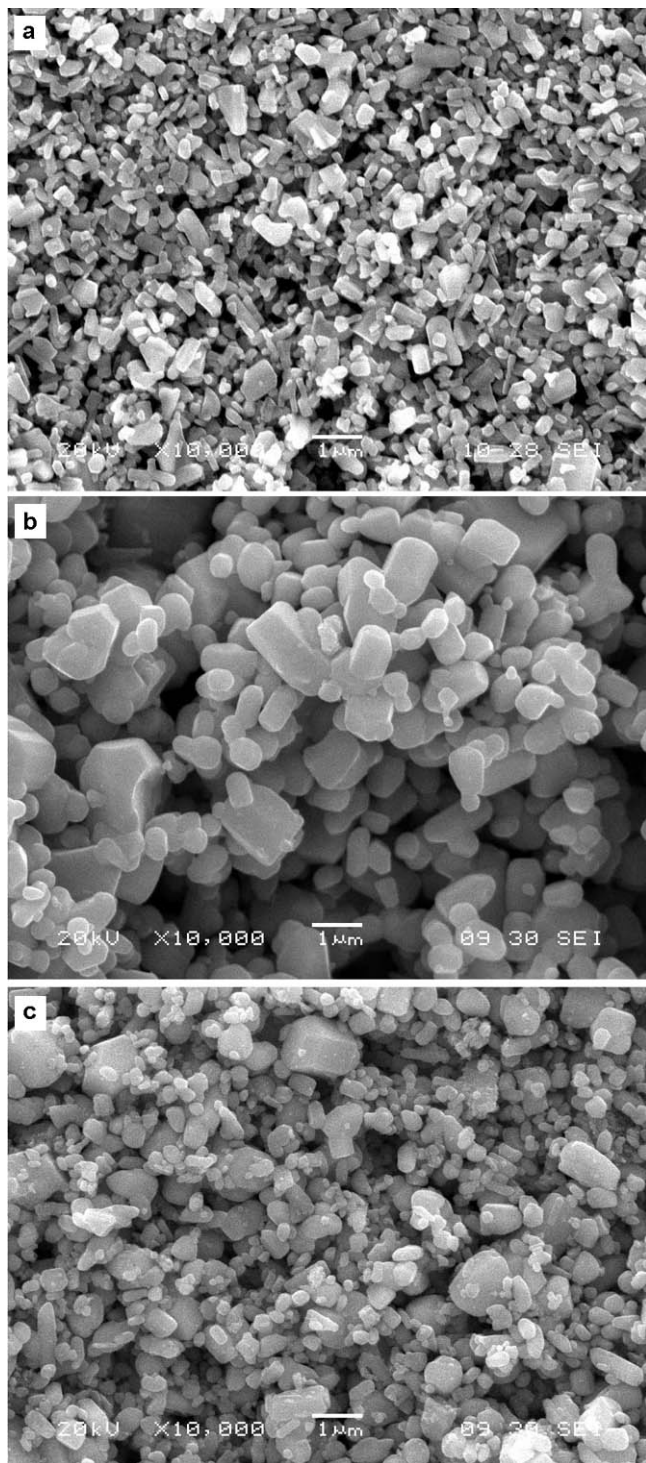


Figure 1. XRD of (a) unmodified ZnO and (b)  $\text{Al}_2\text{O}_3$ -doped (1 wt%) ZnO.

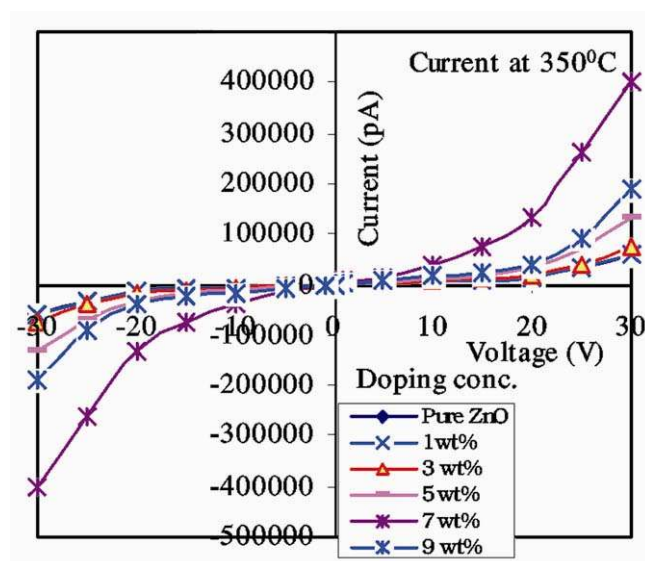
#### 4.2 Electrical conductivity

Figure 4 shows the variation of log (conductivity) with temperature. The conductivity values of all samples in-



**Figure 2.** Micrographs of pure and Al<sub>2</sub>O<sub>3</sub>-doped ZnO samples: (a) pure ZnO, (b) 1 wt% Al<sub>2</sub>O<sub>3</sub>-doped ZnO and (c) 7 wt% Al<sub>2</sub>O<sub>3</sub>-doped ZnO.

crease with operating temperature. The increase in conductivity with increasing temperature could be attributed to negative temperature coefficient of resistance and semi-conducting nature of the Al<sub>2</sub>O<sub>3</sub>-doped ZnO. It is observed from figure 4 that the electrical conductivities of the pure and Al<sub>2</sub>O<sub>3</sub>-doped ZnO films are nearly linear in the temperature range from 100–300°C in air ambient. Pure ZnO has only one kind of grains arranged uniformly. The modified films cause the formation of heterogeneous inter-grain boundaries of Al<sub>2</sub>O<sub>3</sub> and ZnO grains.



**Figure 3.** *I*-*V* characteristics of Al<sub>2</sub>O<sub>3</sub> doped ZnO films.

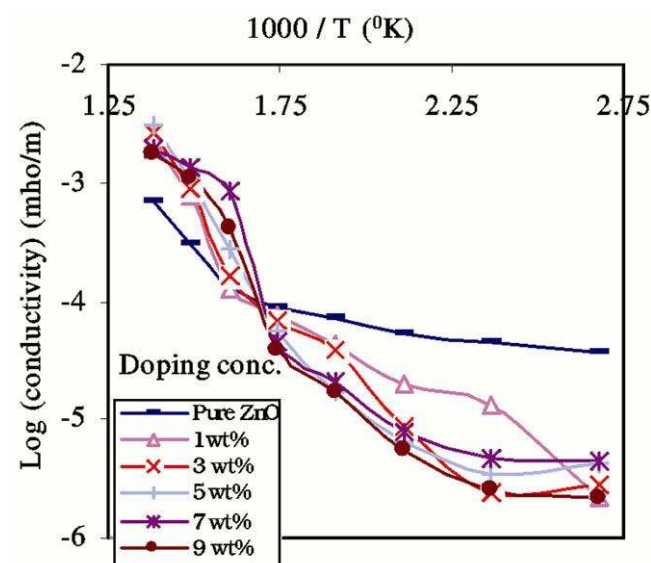


**Figure 4.** Conductivity-temperature profile of Al<sub>2</sub>O<sub>3</sub>-doped ZnO films.

5. Sensing performance of sensor

5.1 Gas response, selectivity, response and recovery time

The relative response (*S*) to a target gas is defined as the ratio of the change in conductance of a sample upon exposure of the gas to the original conductance in air. The relation for *S* is given as

$$S = \frac{G_g - G_a}{G_a}$$

where *G<sub>a</sub>* is the conductance in air and *G<sub>g</sub>* the conductance in a sample gas.

Specificity or selectivity is defined as the ability of a sensor to respond to a certain gas in the presence of different gases. Response time (RST) is defined as the time needed for a sensor to attain 90% of the maximum increase in conductance on exposure to the target gas.

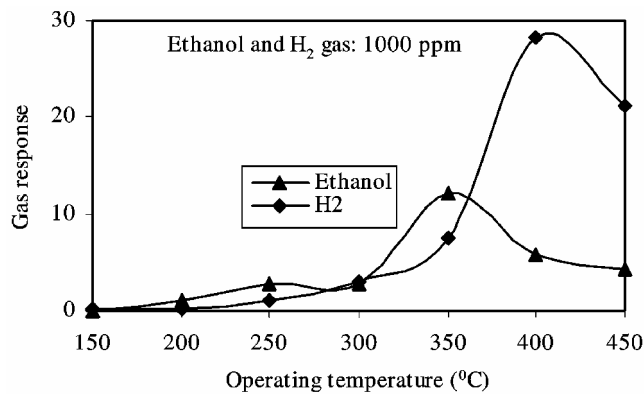


Figure 5. Variation of gas responses of pure ZnO thick film with temperature.

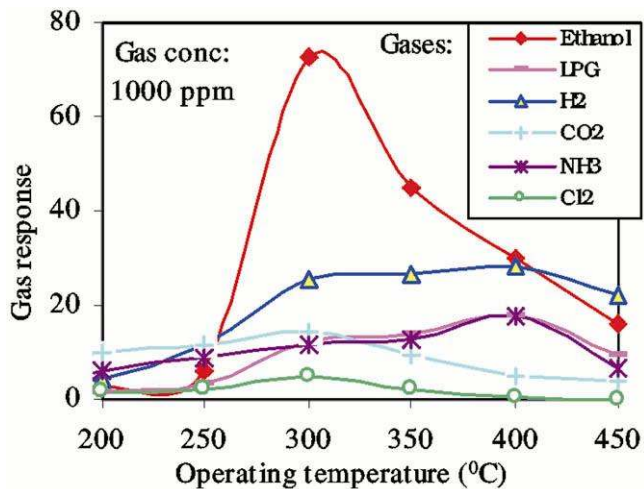


Figure 6. Variation of different gas responses with operating temperatures.

Recovery time (RCT) is the time taken to get back 90% of the original conductance in air.

5.2 Sensing performance of pure ZnO thick films

Figure 5 shows the variation of ethanol and H<sub>2</sub> gas (1000 ppm each) responses of pure ZnO with operating temperature. The responses of pure ZnO thick film to both H<sub>2</sub> and C<sub>2</sub>H<sub>5</sub>OH were observed to increase with operating temperature, reach to their respective maxima and then decreased with further increase in operating temperature. The responses of pure ZnO to ethanol and H<sub>2</sub> were found to be 12 and 28 at 350°C and 400°C, respectively. The lower selectivity to a particular gas against different gases is the main drawback of pure ZnO thick films.

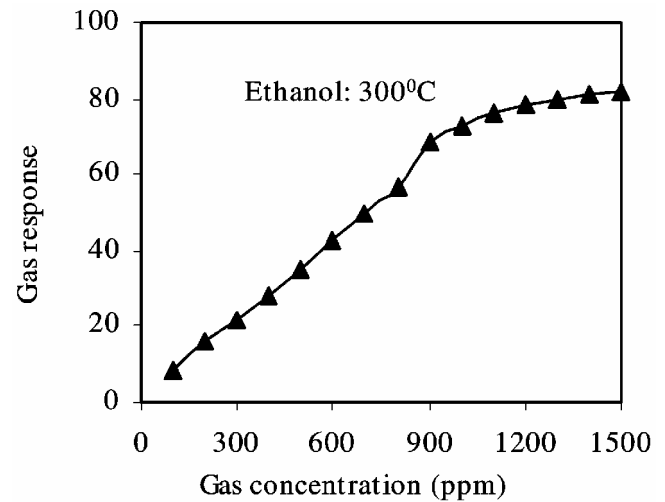


Figure 7. Variation of gas response with gas concentration.

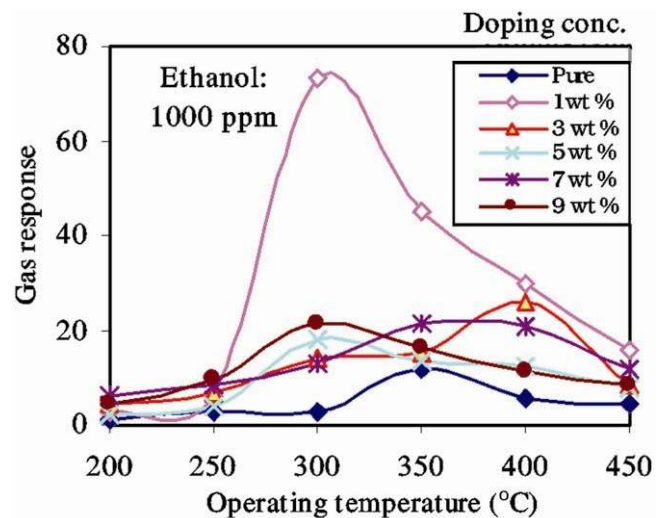


Figure 8. Variation of gas response with operating temperature.



### 5.3 Sensing performance of Al<sub>2</sub>O<sub>3</sub> doped ZnO thick films

**5.3a Response of sensor to various gases:** The variation of different gas responses of Al<sub>2</sub>O<sub>3</sub>-doped ZnO (1 wt%) sample with operating temperatures is represented in figure 6. It is clear from the figure that the gas responses go on increasing, reach to their respective maxima and decreased further with increase in operating temperatures. It is clear from the figure that the Al<sub>2</sub>O<sub>3</sub>-doped ZnO (1 wt%) sample shows the largest response to ethanol vapours at 300°C.

**5.3b Active region of sensor:** Figure 7 depicts the variation of gas response of Al<sub>2</sub>O<sub>3</sub>-doped ZnO sample with ethanol vapour concentrations. It is clear from the figure that the gas response goes on increasing linearly

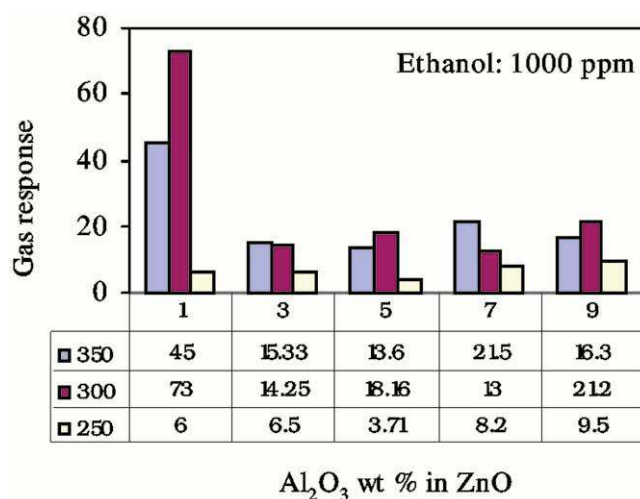


**Figure 9.** Variation of gas response with wt% of Al<sub>2</sub>O<sub>3</sub> in ZnO samples.

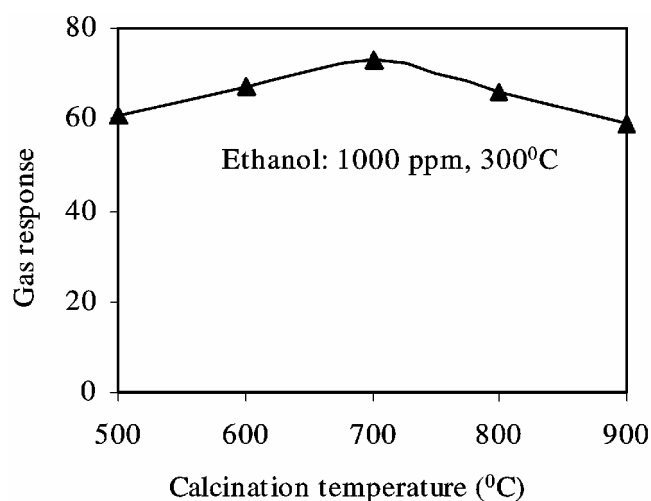


**Figure 10.** Variation of gas response with calcination temperature.

with gas concentration up to 1000 ppm and saturated beyond it. The rate of increase in gas response was relatively larger up to 1000 ppm. The monolayer of the gas molecules formed on the surface could cover the whole surface of the film. The gas molecules from that layer would reach the surface active sites of the film. The excess gas molecules would remain idle and would not reach surface active sites of the sensor. So, the gas response at higher concentrations of the gas is not expected to increase further in large extent. Thus, the active region of the sensor would be up to 1000 ppm.

**5.3c Effect of operating temperature:** Figure 8 depicts the variation of gas response to ethanol vapours (1000 ppm) with operating temperature. The largest response of Al<sub>2</sub>O<sub>3</sub>-doped (1 wt%) ZnO to ethanol was observed to be 73 at 300°C. The response could be attributed to the adsorption-desorption type of sensing mechanism. The amount of oxygen adsorbed on the surface would depend on the number of Al<sub>2</sub>O<sub>3</sub> misfits on the ZnO surface and operating temperature.

**5.3d Effect of doping concentration:** It is clear from the observations that the change in wt % of Al<sub>2</sub>O<sub>3</sub> doped into ZnO changes the sensing habits and therefore, it could sense different gases at different levels of doping. Figure 9 indicates the C<sub>2</sub>H<sub>5</sub>OH gas response as a function of the amount (wt%) of Al<sub>2</sub>O<sub>3</sub> in ZnO. Al<sub>2</sub>O<sub>3</sub> (1 wt%) doped ZnO sample was observed to be the most sensitive to ethanol (73, 300°C). The higher response may be attributed to the optimum porosity and largest effective surface area available to react the gas and appropriate number of Al<sub>2</sub>O<sub>3</sub> misfits to adsorb the oxygen which in turn would oxidize the exposed gas.

**5.3e Effect of calcination temperature:** Figure 10 represents the variation of ethanol response with calcination temperature of Al<sub>2</sub>O<sub>3</sub>-doped ZnO films on alumina substrates. It shows that the gas response increases with calcination temperature, reaches the maximum for the film calcined at 700°C for 12 h and falls with a further increase in calcination temperature. It is well known that the grain size of the film increases with calcination temperature. At 700°C, the grain size would be optimum to get the largest effective surface area and critical porosity which would have favoured and enhanced the gas response to achieve its maximum. At higher temperatures (>700°C) the average grain size would increase and therefore, the intergranular potential barrier increases. This decreases the gas response.

**5.3f Selectivity factor of Al<sub>2</sub>O<sub>3</sub>-doped ZnO for various gases:** It is observed from figure 11 that the Al<sub>2</sub>O<sub>3</sub>-doped ZnO sensor gives maximum response to ethanol vapours (1000 ppm) at 300°C. The sensor showed highest selectivity for ethanol against all other tested gases: NH<sub>3</sub>, LPG, CO<sub>2</sub> and Cl<sub>2</sub>.

5.3g *Response and recovery time*: The response and recovery of Al<sub>2</sub>O<sub>3</sub> doped ZnO (1 wt%) sensor are represented in figure 12. The response was quick (~18 s) to 1000 ppm of ethanol, while the recovery was fast (~40 s). The quick response may be due to faster oxidation of gas. The negligible quantity of the surface reaction product and its high volatility explains its quick response and fast recovery to its initial chemical status.

## 6. Discussion

The working principle of the thick film semiconducting gas sensors is based on the change of the electronic conductivity of the semiconducting material upon exposure to ethanol vapours. The interaction of ethanol gas molecules with surface of thick film causes the transfer of electrons between semiconducting surface and adsorbates.

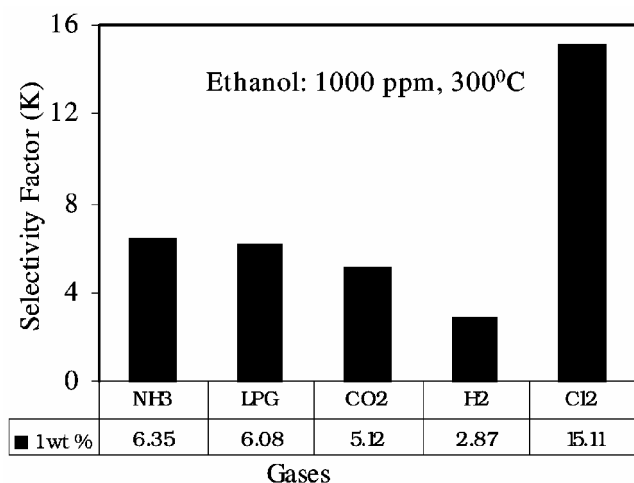


Figure 11. Selectivity factor of the sensor for various gases.

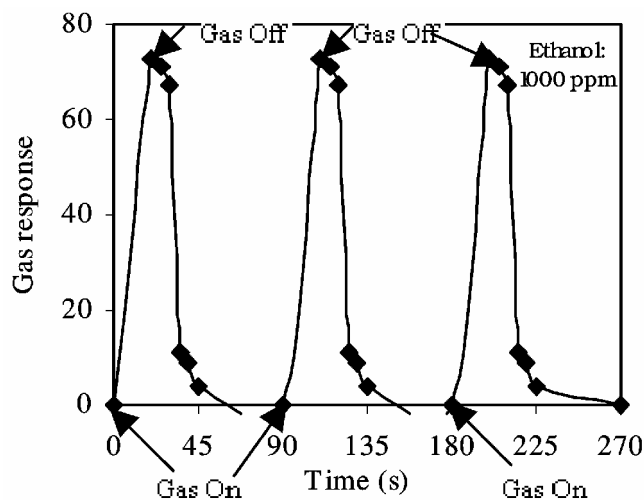
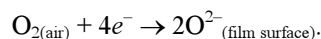


Figure 12. Response and recovery of Al<sub>2</sub>O<sub>3</sub> doped ZnO sample.

The atmospheric oxygen molecules, O<sub>2</sub>, are adsorbed on the surface of the thick film. They capture the electrons from conduction band of the thick film material as

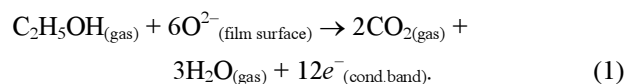


It results in decreasing electronic conductivity of the film. The mass% of Zn and O in each sample was not as per the stoichiometric proportion and all samples were observed to be oxygen-deficient. This deficiency gets reduced (though in less extent) due to adsorption of atmospheric molecular oxygen. This helps in decreasing electronic conductivity of the film. Upon exposure, ethanol molecules get oxidized with the adsorbed oxygen ions, by following a series of intermediate stages, producing CO<sub>2</sub> and H<sub>2</sub>O. This results in evolving oxygen as electrically neutral atoms trapping behind the negative charges (electrons) on the film surface. Upon exposure of ethanol gas, the energy released in decomposition of ethanol molecules would be sufficient for trapped electrons to jump into the conduction band of modified ZnO, resulting in increase in the conductivity of the thick film of modified ZnO.

The drastic increase in conductivity of Al<sub>2</sub>O<sub>3</sub>-doped ZnO could be attributed to the charge-carrier generation mechanism resulting from the electronic defects and can be described in the Kroger-Vink (Kwon *et al* 1995) notation as



These generated electrons and donor levels in the energy band gap of ZnO will contribute to an increase in conductivity. When ethanol reacts with oxygen, a complex series of reactions take place, ultimately converting the ethanol to carbon dioxide and water as



This shows an *n*-type conduction mechanism. Thus on oxidation, single molecule of ethanol liberates twelve electrons (1) in conduction band and results in increase in conductivity of the sensor. Increase in operating temperature causes oxidation of large number of ethanol molecules, thus producing very large number of electrons. Therefore, conductivity increases to a large extent. This is the reason why the gas response increases with operating temperature. The thermal energy (temperature) at which the gas response is maximum, is the actual thermal energy needed to activate the material for progress in reaction. However, the response decreases at higher operating temperature, as the oxygen adsorbates are desorbed from the surface of the sensor (Windichamann and Mark 1979). Also, at higher temperature, the carrier concentration increases due to intrinsic thermal excitation and the Debye length decreases. This may be one of the reasons for decreased gas response at higher temperature (Mizsei 1995).

## 7. Conclusions

From the results obtained, following conclusions can be made for the sensing performance of the sensors.

(I) Pure zinc oxide showed low response to ethanol vapours.

(II) Among all other additives tested, Al<sub>2</sub>O<sub>3</sub> in ZnO is outstanding in promoting the ethanol gas sensing mechanism.

(III) 1 wt% Al<sub>2</sub>O<sub>3</sub> doped into ZnO was found to be optimum and showed highest response to ethanol vapours at 300°C.

(IV) Al<sub>2</sub>O<sub>3</sub>-doped ZnO has the potential of fabricating the ethanol vapours sensor.

(V) The sensor showed very rapid response and recovery to ethanol vapours.

(VI) The sensor has good selectivity to ethanol against LPG, NH<sub>3</sub>, CO<sub>2</sub>, Cl<sub>2</sub> and H<sub>2</sub> at 300°C.

## References

- Chang J F, Kuo H H, Leu I C and Hon M H 2002 *Sens. Actuators* **B84** 258
- Chaudhary V A, Mulla I S and Vijayamohan K 1999 *Sens. Actuators* **B55** 127
- Jayaraman V, Gnanasekar K, Prabhu E, Gnanasekaran T and Periaswami G 1999 *Sens. Actuators* **B55** 175
- Kwon C H, Hong H K, Yun D H, Lee K, Kim S T, Roh Y H and Lee B H 1995 *Sens. Actuators* **B24–25** 610
- Lin F, Takao Y, Shimizu Y and Egashira M 1995 *Sens. Actuators* **B25** 843
- Matsushima S, Maekawa T, Tamaki J, Miura N and Yamazoe N 1989 *Chem. Lett.* 845
- Miremadi B K, Singh R C, Chen Z, Morrison S R and Colbow K 1994 *Sens. Actuators* **B21** 1
- Miyayama M, Hikita K, Uozumi G and Yanagida H 1995 *Sens. Actuators* **B24–25** 383
- Mizsei J 1995 *Sens. Actuators* **B23** 173
- Moseley P T 1992 *Sens. Actuators* **B6** 149
- Nanto H, Kawai T and Tsubakino S 1993 *Proc. symposium on chemical sensors II*, in *Sensor group proc.* (eds) M Butler *et al* (Pennington, NJ: Electrochem. Soc. Inc.) **93** p. 522
- Patil D R and Patil L A 2006a *Sensors & Transducers* **70** 661
- Patil L A and Patil D R 2006b *Sens. Actuators* **B120** 316
- Pearson S J, Norton D P, Ip K, Heo Y W and Steiner T 2005 *Prog. Mater. Sci.* **50** 293
- Seiyama T and Era F 1971 *Zairyo-Kagaku Jpn* **8** 232
- Seiyama T, Kato A, Fujitshi K and Nagatanui M 1962 *Anal. Chem.* **34** 1502
- Sodhi G S 2002 *Fundamental concepts of environmental chemistry* (New Delhi: Narosa Publishing House) p. 135
- Solomans Graham T W and Fryhle C B 2004 *Organic chemistry* (Singapore: John Wiley and Sons Inc.) 8th edn, p. 497
- Takao Y, Shimizu Y and Egashira M 1989 *Digest of 9th chemical sensor symposium* (Japan: Aoyama Gakuin University) p. 29
- Trivikrama Rao G S and Madhavendra S S 1995 *J. Mater. Sci. Lett.* **14** 529
- Windichamann H and Mark P 1979 *J. Electrochem. Soc.* **126** 627
- Xiangfeng C, Xingqin L and Guangyao M 2000 *Sens. Actuators* **B65** 64